JGR Space Physics

RESEARCH ARTICLE
10.1029/2019JA026553

Acceleration of Ions in Jovian Plasmoids: Does Turbulence Play a Role?

E. A. Kronberg[1,2], E. E. Grigorenko[3,4], A. Malykhin[3], L. Kozak[5], B. Petrenko[5], M. F. Vogt[6], E. Roussos[1], P. Kollmann[7], C. M. Jackman[8], S. Kasahara[9], Kh. V. Malova[3,10], C. Tao[11,12], A. Radioti[13], and A. Masters[14]

[1]Max Planck Institute for Solar System Research, Göttingen, Germany, [2]Department of Earth and Environmental Sciences,Ludwig Maximilian University of Munich, Munich, Germany, [3]Space Research Institute, Russian Academy of Sciences, Moscow, Russia, [4]Moscow Institute of Physics and Technology, Moscow, Russia, [5]Astronomy and Space Physics Department,Kyev Taras Shevchenko University, Kyev, Ukraine, [6]Boston University, Boston, MA, USA, [7]Applied Physics Laboratory, Johns Hopkins University, Baltimore, MD, USA, [8]School of Physics and Astronomy, University of Southampton, Southampton, UK, [9]Department of Earth and Planetary Science,University of Tokyo, Tokyo, Japan, [10]Skobeltsyn Institute of Nuclear Physics, Lomonosov Moscow State University, Moscow, Russia, [11]National Institute of Information and Communications Technology, Koganei, Japan, [12]Department of Geophysics, Tohoku University, Sendai, Japan, [13]Space Sciences, Technologies and Astrophysics Research Institute, LPAP, Université de Liège, Belgium, [14]The Blackett Laboratory, Imperial College London, London, UK

Key Points:
- Ions are accelerated effectively by plasmoids in the Jovian magnetosphere
- Plasmoids with higher electromagnetic turbulence lead to stronger acceleration of oxygen and sulfur ions
- Acceleration of hydrogen ions is not correlated with wave power, possibly because of limitations in observations

Correspondence to:
E. A. Kronberg,
kronberg@mps.mpg.de

Citation:
Kronberg, E. A., Grigorenko, E. E., Malykhin, A. Y., Kozak, L., Petrenko, B., Vogt, M. F., et al. (2019). Acceleration of ions in Jovian plasmoids: Does turbulence play a role? *Journal of Geophysical Research: Space Physics*, *124*. https://doi.org/10.1029/2019JA026553

Received 26 JAN 2019
Accepted 8 JUN 2019
Accepted article online 27 JUN 2019

Abstract The dissipation processes which transform electromagnetic energy into kinetic particle energy in space plasmas are still not fully understood. Of particular interest is the distribution of the dissipated energy among different species of charged particles. The Jovian magnetosphere is a unique laboratory to study this question because outflowing ions from the moon Io create a high diversity in ion species. In this work, we use multispecies ion observations and magnetic field measurements by the Galileo spacecraft. We limit our study to observations of plasmoids in the Jovian magnetotail, because there is strong ion acceleration in these structures. Our model predicts that electromagnetic turbulence in plasmoids plays an essential role in the acceleration of oxygen, sulfur, and hydrogen ions. The observations show a decrease of the oxygen and sulfur energy spectral index γ at ~30 to ~400 keV/nuc with the wave power indicating an energy transfer from electromagnetic waves to particles, in agreement with the model. The wave power threshold for effective acceleration is of the order of 10 nT^2Hz^{-1}, as in terrestrial plasmoids. However, this is not observed for hydrogen ions, implying that processes other than wave-particle interaction are more important for the acceleration of these ions or that the time and energy resolution of the observations is too coarse. The results are expected to be confirmed by improved plasma measurements by the Juno spacecraft.

1. Introduction

Studying the magnetospheres of planets other than Earth can bring us additional insights in solving the puzzle of energization related to turbulence. The Jovian magnetosphere is an excellent laboratory to study acceleration of multispecies plasma. The moon Io delivers cold heavy ions into the magnetosphere. Therefore, iogenic ions such as O^+, O^{++}, S^{++}, and S^{+++} dominate in the inner magnetosphere of Jupiter (e.g., Clark et al., 2016; Geiss et al., 1992). However, in the outer magnetosphere the ions of the solar wind origin such as H^+ and He^{++} become more abundant (e.g., Haggerty et al., 2009).

Relatively cold solar wind ions (1 keV) and ions of internal origin (ionosphere, moons) with energies ~10–100 eV enter the planetary magnetospheres via various processes. On closed field lines, or in the magnetotail plasma sheet, the ions become energetic. Particles may have energies ranging from tens to hundreds of kiloelectron volts. The mechanism by which ions get accelerated from thermal to the suprathermal energies is unknown. According to the estimations by Bagenal and Delamere (2011), a rapidly rotating Jovian massive magnetodisk dominated by oxygen and sulfur needs an additional total input of 3–16 TW to account for the observed energy density. There are many acceleration mechanisms responsible for the ion energization in the magnetotail. These include adiabatic processes, such as first Fermi and betatron acceleration, as well as nonadiabatic processes, such as (1) large-scale convection electric field during “demagnetization”

near the current sheet center (e.g., Lyons & Speiser, 1982) and (2) inductive electric fields generated during transient processes such as the formation of a magnetic X-line (e.g., Luo et al., 2014; Wygant et al., 2005), dipolarization fronts (e.g., Delcourt & Sauvaud, 1994; Greco et al., 2015), plasmoids (e.g., Zong et al., 1997), and electromagnetic turbulence (e.g., Catapano et al., 2016) as shown for the terrestrial magnetosphere.

It is still unclear how the electromagnetic turbulence dissipates in space plasmas and how effective this energy transformation is, especially in multispecies plasmas. This question is still controversial in the terrestrial magnetosphere. On one side Catapano et al. (2016) using test particle simulations have modeled the acceleration of ions by stochastic electromagnetic turbulence in the terrestrial magnetotail and found that the most effectively accelerated ion is He^{++}, compared to protons and O^{+} which are accelerated with equal efficiency. Conversely, in observations of the terrestrial magnetotail the effectiveness of the ion energization is the strongest for the oxygen and the weakest for the protons (Kronberg et al., 2017). However, in observations multiple effects such as dipolarizations and turbulence are present, and therefore, it is important to separate them.

The acceleration to high energies is usually associated with spatially confined structures such as fast planetward moving plasma flows, plasmoids, and flux ropes because they generate strong electric fields in planetary magnetotails. It is, therefore, reasonable to focus on one of these phenomena. In the terrestrial magnetosphere this was done for the dipolarization fronts by Ono et al. (2009), Grigorenko et al. (2017), Malykhin et al. (2018), and Parkhomenko et al. (2018). The main result of these investigations is that the charged particles are effectively accelerated by the electromagnetic fluctuations at the frequency corresponding to the gyrofrequency of the respective charged particle. In terrestrial plasmoids the same effect was observed by Grigorenko et al. (2015). This study has shown that a certain minimum of the wave power is necessary to accelerate helium and oxygen ions. It was also shown that O^{+} ions are accelerated more efficiently than hydrogen and helium.

Jupiter's magnetosphere, similar to the terrestrial one, undergoes reconfiguration processes in the magnetotail (Woch et al., 1999; Kronberg et al., 2005; Kronberg, Glassmeier, et al., 2008). The magnetic field and particle signatures of these processes are somewhat similar to those of terrestrial substorms, and they can lead to particle acceleration. The effective acceleration by inductive electric fields generated during transient processes in the magnetotail was shown by Radioti et al. (2007), acceleration related to the formation of a magnetic X-line by Kronberg et al. (2012), and acceleration at the dipolarization fronts by Kasahara et al. (2011). However, these processes are unlike terrestrial substorms in that they are mainly triggered by an internal source, mass loading from the moon Io and can be periodic on timescales of 2.5–4 days (Kronberg et al., 2009; Woch et al., 1998; Vasyliūnas, 1983).

The plasma turbulence in the Jovian magnetosphere shows spectral breaks at the gyrofrequencies of heavy ions (Tao et al., 2015). This may indicate the conversion of the electromagnetic energy to the kinetic energy of ions. They also found that in the magnetotail (>80 R_J) the wave power is higher in the dawn region where most of the fast plasma flows are observed (Krupp et al., 2001).

We here investigate the effectiveness of ion acceleration to suprathermal energies for multiple species and for different levels of turbulence in plasmoids of the Jovian magnetotail. The characteristics of plasmoids such as their speed, size, and associated electric field were studied by Kronberg, Woch, et al. (2008) and Vogt et al. (2014). However, the acceleration processes associated with these structures and related electromagnetic fluctuations were not considered before. In section 2 we describe the data and methodology used in this study. Then we present two plasmoid events and statistical results on acceleration in plasmoids based on Galileo observations in section 3. In section 4 we model the particle dynamics in a typical Jovian plasmoid using test particle simulations. The results from observations and simulations are discussed in section 5.

2. Instrumentation and Methodology

To investigate the Jovian plasmoids in the magnetotail, we used data from instruments onboard the Galileo spacecraft. Ion fluxes were measured by the Energetic Particle Detector (EPD; Williams et al., 1992). The EPD instrument provides the ion fluxes in the range from 22 keV/nuc to 55 MeV/nuc. The fluxes are measured almost isotropically with a time resolution of 3–11 min depending on the transmission rate to Earth. The magnetic field was measured by the fluxgate magnetometer with a typical temporal resolution

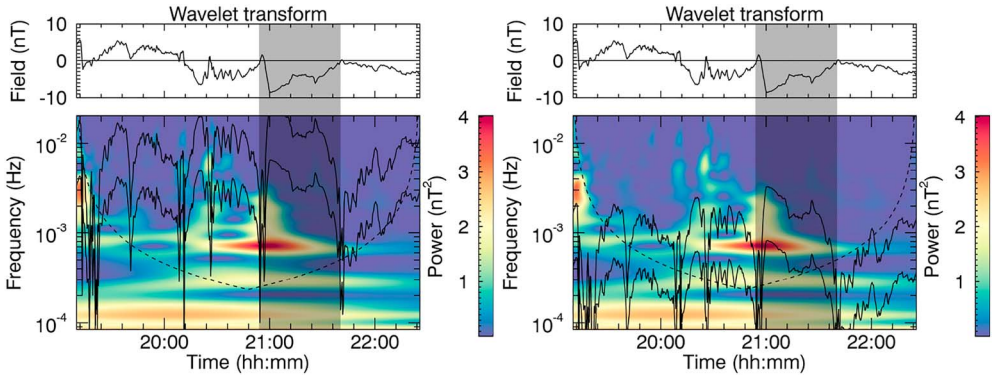

Figure 1. (top row) Time series of the magnetic field (component B_θ) observed by Galileo used for the wavelet analysis and (bottom row) its continuous wavelet power spectrum for the event on 28 September 1996. Black lines on the wavelet power spectrum indicate the frequencies at $0.1f_{gi}$ and $0.4f_{gi}$ for the He^{++} (left column) and O^+ (right column) ions. The cone of influence where edge effects become considerable is indicated by dashed line. Gray bar indicates time of plasmoid based on B_θ most close approaching "0" value at the start/end of the plasmoid.

of 24 s (Kivelson et al., 1992). The electron number density, n_e, is derived from the cutoff frequency of the electromagnetic waves measured by the Plasma Wave Spectrometer (PWS; Gurnett et al., 1992).

We select events based on plasmoids identified by Vogt et al. (2014). In section 3.2 of Vogt et al. (2014) one can find details on the selection criteria. From 43 plasmoids in the list we have taken those during which EPD data were available. In total we identified 14 plasmoids. All these plasmoids overlap with plasmoids identified by Kronberg, Woch, et al. (2008).

We used wavelet transformations (Torrence & Compo, 1998) to analyze the frequency and wave power of fluctuations in the meridional component of the magnetic field, B_θ, which displays a bipolar signature (field dipolarization and reversal) during a plasmoid. The plasmoids propagate tailward with the bulk speed of 350–500 km/s (Kronberg, Woch, et al., 2008). Therefore, before analyzing the wave power of magnetic fluctuations within a plasmoid, we have to subtract the Doppler shift. Following Grigorenko et al. (2015), in the plasma rest frame we use formula $f_0 = f_{SC} - f_{SC}\frac{V}{V_{PH}}$, where f_{SC} is the observed frequency of the magnetic field fluctuations, V is the bulk velocity of the plasmoid, which is directed mainly tailward, and V_{PH} is a wave phase velocity. The Galileo spacecraft does not measure the electric field, which could help us to estimate $v_{PH} \sim \delta E_y/\delta B_z$, and thus, we must use another approach. We assume that the magnetic field fluctuations are related to the Alfvén waves. Kronberg, Woch, et al. (2008) have estimated the Alfvén Mach number of the propagating plasmoids, M_a, for a data set of 14 examples and found that the plasmoid propagation speed is nearly Alfvénic. The Alfvén Mach number is calculated as $M_a = V/V_a$, where the speed of a plasmoid, V, is defined using a technique described in Krupp et al. (2001) and V_a is the Alfvén speed. The Alfvén speed is calculated using the following expression from Goedbloed and Poedts (2004): $V_a = 2.8 \times 10^{16}\sqrt{Z/AB}/\sqrt{n}$ with $n \equiv n_e \simeq Zn_i$, where n_e is the electron density, n_i is the ion density, Z is the ion charge number, A is the ion mass number, and B is the magnetic field in the lobe region. The values of the electron number density n_e are derived from Galileo PWS data . The average ion mass number A is assumed to be 16 and the ion charge $Z = +2$; see details in Kronberg, Woch, et al. (2008).

Those plasmoids which have the Alfvén Mach number higher or equal to 1 are not considered in our study, as the f_0 becomes negative. The average value of the Mach number for the sub-Alfvénic plasmoids is approximately 0.8. Therefore, the observed frequency range f_{SC} is shifted in the plasma rest frame to lower frequencies: $f_0 = f_{SC} - 0.8f_{SC} = 0.2f_{SC}$. The most probable range of the Alfvén Mach number is between 0.6 and 0.9. From this we have the variation of the frequency range between $f_0 = f_{SC} - 0.6f_{SC} = 0.4f_{SC}$ and $f_0 = f_{SC} - 0.9f_{SC} = 0.1f_{SC}$. According to Grigorenko et al. (2015), the ions interact most effectively with waves at the corresponding ion gyrofrequency. The integrated wavelet intensity between the frequencies, $0.1f_{gi}$ and $0.4f_{gi}$, where f_{gi} is ion gyrofrequency, is used in further analysis. This allows us to take into account the large variation of the possible plasmoid velocities relatively to the Alfvén speed.

In Figure 1 we show the variation of the B_θ component of the magnetic field and wavelet analysis for the plasmoid event on 28 September 1996 and considered in more details in section 3 and Figure 3. Black

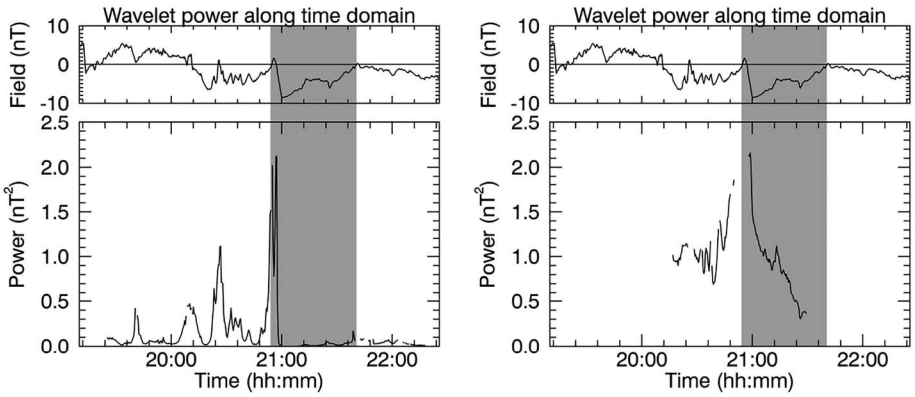

Figure 2. (top row) Time series of the magnetic field (component B_θ) observed by Galileo used for the wavelet analysis and (bottom row) the integrated wavelet power between $0.1f_{gi}$ and $0.4f_{gi}$ indicated in Figure 1 for the He^{++} (left column) and O^+ (right column) for the event on 28 September 1996. The power during times when the edge effects become important and/or the frequency boundaries are beyond allowed range is shown as data gap. Gray bar indicates time of plasmoid based on B_θ most close approaching "0" value at the start/end of the plasmoid.

lines on the wavelet power spectrum indicate the frequencies at $0.1f_{gi}$ and $0.4f_{gi}$ for the He^{++} (left) and O^+ (right) ions. The wavelet power is integrated between these two frequency bands. The derived wavelet powers for the He^{++} and O^+ frequency bands are shown in Figure 2. Calculation of wavelet power is limited because of (1) cone of influence, (2) upper-frequency boundary $0.4f_{gi}$ is higher than Nyquist frequency, and (3) low-frequency boundary $0.1f_{gi}$ is lower than the lowest frequency in wavelet transform. When one of these three conditions was fulfilled, the data point was discarded from the data used in further analysis; see Figure 2. For each reliable measurement, the wavelet power (nT^2) is transformed into the wave

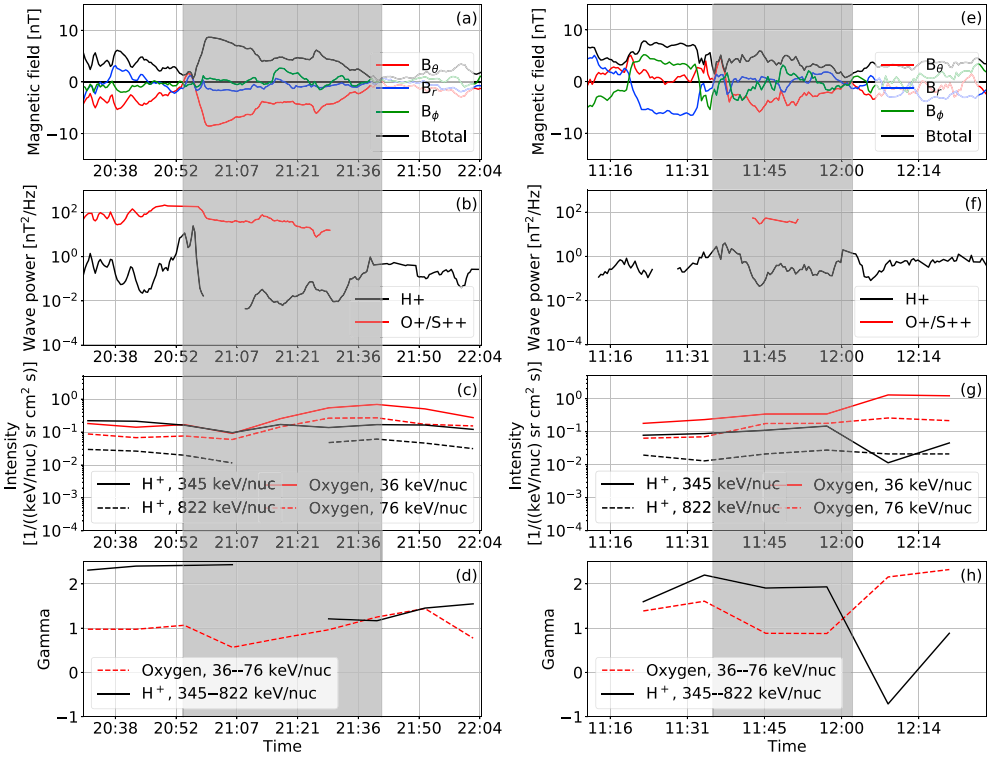

Figure 3. The magnetic field components (a, e), wave power (b, f), ion intensity (c, g), and spectral index γ (d, h) for a quiet plasmoid observed on 28 September 1996 (left column) and a plasmoid associated with turbulence observed on 10 June 1997 (right column). Gray bar indicates time of plasmoid based on B_θ most close approaching "0" value at the start/end of the plasmoid.

Table 1

Date	Start time	End time	Duration, min
1996-Oct-01	17:02:02.795	17:12:50.194	11
1996-Oct-03	16:41:38.689	16:54:50.089	13
1996-Oct-05	09:44:26.598	13:48:02.537	244
1996-Oct-18	17:08:25.890	17:22:01.290	14
1996-Sep-20	13:22:27.388	13:30:27.387	8
1996-Sep-20	18:44:03.376	19:53:38.774	70
1996-Sep-23	00:34:51.256	00:44:51.256	10
1996-Sep-24	08:12:03.186	09:53:39.185	102
1996-Sep-26	09:21:39.077	12:08:03.077	166
1996-Sep-28	20:55:38.948	21:40:26.945	105
1997-Jun-07	04:40:38.560	05:15:50.559	35
1997-Jun-10	11:37:26.390	12:15:02.390	38
1997-Jun-14	01:34:14.206	02:44:37.605	70
1997-Oct-21	16:55:02.523	17:14:14.523	19

Note. Date is formatted as YYYY-MM-DD.

power (nT^2 Hz^{-1}). To do this, we divide squared wavelet power on the frequency band width equal to $0.4f_{gi}$–$0.1f_{gi}$=$0.3f_{gi}$. For calculations of ion gyrofrequency we used simultaneous magnetic field observations for each measurement.

Unfortunately, the observations for helium are shown to be not very robust. The ion data are corrected for the radiation background contamination. After this correction, we had an insufficient amount of reliable observations of helium for our analysis. Instead, we further investigate proton intensities. However, for them we cannot directly calculate the wave power because of the resolution of the magnetic field. We assume in this case that the wave power was obeying a power law with a spectral index $k = -2.3$ (Tao et al., 2015). From this we can derive the wave power using the expression $W_p = W_{He^{++}}(f_p/f_{He^{++}})^k$, where W_i is the wave power at corresponding ion frequency.

Our analysis has shown that part of the selected plasmoids has timescales comparable to the Doppler-shifted gyroperiod of oxygen ion. An example of such plasmoid is shown in Figure 1. The plasmoid was defined by Vogt et al. (2014) from 20:55 to 21:00 UT. Therefore, its duration of 5 min is comparable with the oxygen gyroperiod on scales of ~5 to 23 min. In such structures we cannot investigate influence of the magnetic field turbulence on the acceleration. We, therefore, included in definition of the plasmoid also the post plasmoid plasma sheet (PPPS; Richardson et al., 1987), the long structures surrounding a plasmoid between two X-lines. Previous observations show that these structures are associated with strong ion acceleration (Kronberg et al., 2005, Kronberg, Glassmeier, et al., 2008). The plasmoid in Figure 3 in our study starts at 20:55 and ends at 21:40 UT, with duration period of 105 min. The end interval is defined at time when negative B_θ most closely approaches 0. The time intervals of plasmoid observations and their duration are listed in Table 1.

3. Observations

We conduct a statistical analysis of 14 plasmoids observed in the Jovian magnetotail. Figure 3 shows observations of two plasmoids. They are seen as a bipolar fluctuation of the meridional magnetic field component shown by red lines in panels (a) and (e). The time of plasmoid observations is indicated by the gray transparent bars. The plasmoid on the left side is associated with low level of turbulence represented by the wave power, and on the right side is associated with higher level of turbulence at least at hydrogen gyrofrequency (see panels [b] and [f]). The increase of intensities of oxygen has been observed during the plasmoids (see panels [c] and [g]). For hydrogen, the increase is seen during the plasmoid associated with turbulence. Intensities of sulfur ions (not shown here) change very similarly to intensities of oxygen ions during these two events. Energy spectral index γ for oxygen is on average lower during the observation of plasmoids (see panels [d] and [h]). Energy spectral index γ indicates a slope of the ion energy spectrum $I \sim E^{-\gamma}$, where I is the ion intensity and E is the energy of the ions. This implies acceleration of oxygen ions. The decrease of aver-

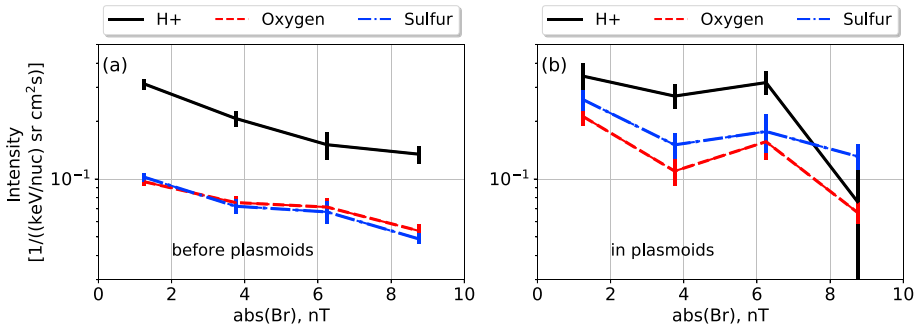

Figure 4. Dependence of the ion intensity on the vicinity to the current sheet center represented by the B_r magnetic field component (a) during observations 25 min before a plasmoid and (b) during plasmoids. Different lines indicate intensities for hydrogen at 345–822 keV/nuc (black solid line), oxygen at 51–112 keV/nuc (red dashed line) and sulfur 62–310 keV/nuc (blue dash-dotted line). The error bars represent the 95% confidence intervals.

age value is stronger during a plasmoid associated with turbulence. Further, we will conduct a statistical analysis on the relation between the ion intensities and spectral index γ on the wave power.

We check if the ion intensity in 14 selected plasmoids increases relatively to intensities before plasmoids. The intensity of ions may depend on the vicinity to the current sheet center. The vicinity to the current sheet center can be represented by the magnetic field component B_r. It is equal to zero in the current sheet center. Henceforth, we resample the ion intensities to compare them with the magnetic field measurements. After defining uniformly spaced ranges of the magnetic field strength, we calculate the means of the intensities associated with these ranges for time intervals 25 min before plasmoids and in plasmoids. The 25 min are chosen in order to have at least two spins of particle measurements but not longer to minimize influence of other effects. Figure 4 indicates that the ion intensity significantly changes with the distance from the current sheet center. Comparing the ion intensities during plasmoids (shown in Figure 4b) to the ion intensities 25 min before plasmoids (Figure 4a), we note a statistically significant increase of the ion intensities during plasmoids (confidence intervals do not overlap). The only exception is the proton intensity within $B_r < \pm 2.5$ nT. Here, the intensities during plasmoids are higher but the error bars overlap. This indicates that the ions can be accelerated in plasmoids. The aim of this study is to examine how the wave power of the magnetic field fluctuations in plasmoids affects the acceleration of ions. For further analysis we select observations for $B_r < \pm 2.5$ nT to avoid bias related to location in the plasma sheet. This region is close to the current sheet center and also to the center of the plasmoid.

The dependence of the absolute value of B_r component versus wave power is plotted in Figure 5 for observations 25 min before the plasmoids from Table 1 (left) and during the plasmoids (right). Here we take the same uniformly spaced ranges of the magnetic field strength as in Figure 4 and we calculate the means of the wave power associated with these ranges for time intervals 25 min before plasmoids and in plasmoids. The wave power decreases with distance from the current sheet center in the direction of the lobes. This trend is more prominent for the H^+ band than for O^+ and/or S^{++} band in plasmoids. This is expected because

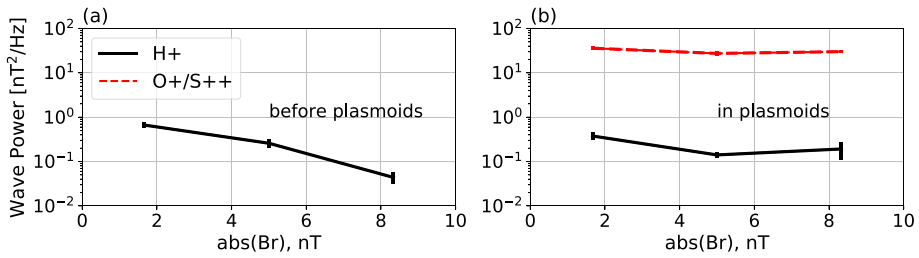

Figure 5. Dependence of the wave power on the vicinity to the current sheet center represented by the B_r magnetic field component (a) during observations 25 min before a plasmoid and (b) during plasmoids. The dependencies are shown for the wave power between 0.1 and 0.4 gyrofrequency of H^+ (black line) and O^+ and/or S^{++} (red dashed line). The error bars represent the 95% confidence intervals.

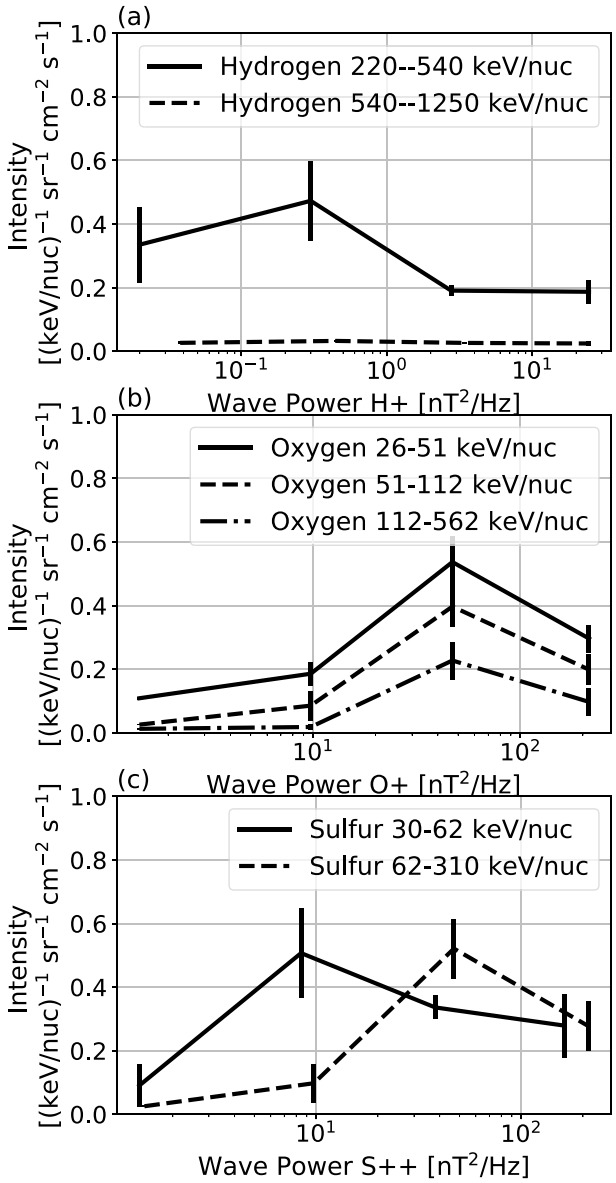

Figure 6. Dependencies of the wave power at frequency bands for (a) H^+, (b) O^+, and (c) S^{++} on the ion intensities. The error bars represent the 95% confidence intervals.

magnetic field fluctuations at O^+ and/or S^{++} band will occupy larger space in the meridional direction due to larger gyroradius.

The wave power for the hydrogen frequency band is significantly lower than those for O^+ and/or S^{++} (see Figure 5). This is in accordance with the nature of turbulence: wave power decreases with frequency. The gyrofrequency of hydrogen is higher than those for O^+ and/or S^{++}.

Inside plasmoids, the wave power shows less dependence on the magnitude of B_r than for observations 25 min before plasmoid (see Figure 5). This is expected as the magnetic field lines in a plasmoid are closed. Assuming that the same wave propagates along a closed line, we will observe the same wave power in the current sheet center and in regions close to the lobe. However, during observations 25 min before the plasmoids, we observed strong dependence of the wave power on the vicinity to the plasma sheet center. The wave power at hydrogen frequency band decreases with distance from the current sheet center. We were not able to derive the O^+ and/or S^{++} frequency band before plasmoids because of limitations in wavelet analysis mentioned in section 2.

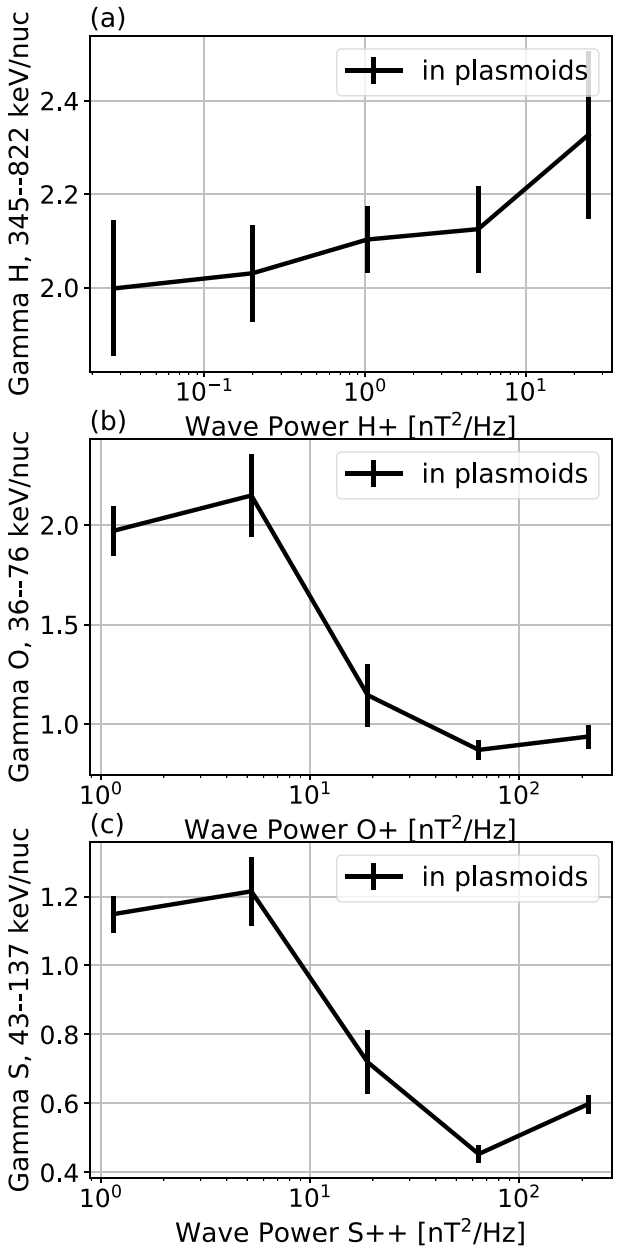

Figure 7. Dependencies of the wave power at frequency bands for (a) H^+, (b) O^+, and (c) S^{++} on the spectral index gamma. The error bars represent the 95% confidence intervals.

The dependencies of the intensities for hydrogen, oxygen, and sulfur ions at different energies on the wave power during observations of plasmoids are shown in Figure 6. The observations show no clear dependence of hydrogen intensities on the wave power. Oxygen and sulfur ion intensities show nonlinear increase with the wave power. The sulfur intensities at two different channels peak at different energies, whereas the oxygen intensities peak at the same wave power. We speculate that the reason for this is the presence of sulfur ions with different charges. The S^{+++} and S^{++++} ions would require less wave power at S^{+++} and S^{++++} frequency bands, respectively, for acceleration. Although these ions are less abundant than S^{++} (Clark et al., 2016), our modeling in section 4 shows that sulfur ions with higher charges are more effectively accelerated.

The dependencies of the spectral index γ for hydrogen, oxygen, and sulfur ions on the wave power during observations of plasmoids are shown in Figure 7. We note decrease of the spectral index γ with the wave power at the frequencies corresponding to the gyrofrequencies of the O^+ and S^{++} ions. This implies that

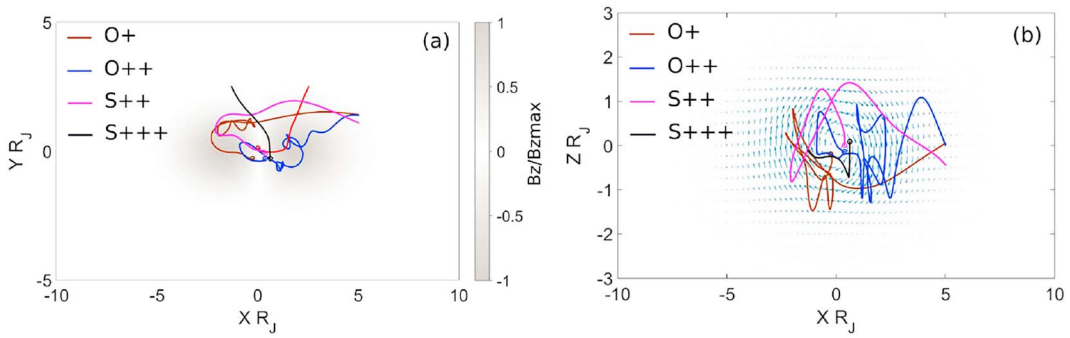

Figure 8. (a) Trajectories of a test O^+, O^{++}, S^{++}, and S^{+++} ions in the plasmoid-like magnetic structure in *XY* plane (a) and *XZ* plane (b). The circles show the start of trajectory for each corresponding species. The background color in plot (a) indicates the strength of the vertical magnetic field component B_z normalized to the $B_{z_{max}}$. The blue arrows in the plot (b) indicate the direction and strength of the B_z component.

the electromagnetic wave energy can be transferred to the ions leading to their acceleration. However, for hydrogen we do not observe a significant dependence. We discuss some possible reasons in section 5.

4. Model

To study ion energization inside the plasmoid-like structures, we analyze the kinetic features of test ion trajectories (H^+, O^+, O^{++}, S^{++}, and S^{+++}) calculated in the prescribed plasmoid-like magnetic configuration

$$\begin{aligned} B_X &= B_0 \tanh(Z/L_Z) + B_P \exp(-(X/L_X + Y/L_Y + Z/L_Z)^2), \\ B_Y &= 0, \\ B_Z &= 0.1B_0 - B_P \exp(-(X/L_X + Y/L_Y + Z/L_Z)^2). \end{aligned} \quad (1)$$

Here $B_0 = 10$ nT is the value of the tangential component of the magnetic field in the outer plasma sheet outside the plasmoid; L_X (~10 R_J; Kronberg, Woch, et al., 2008) and L_Y (~5 R_J, assuming that the plasmoids as at Earth are shorter in *Y* direction; Nakamura et al., 2004) are the radial and azimuthal sizes of the plasmoid respectively; L_Z is the half thickness of the current sheet (~2 R_J; Khurana & Kivelson, 1989; Kronberg et al., 2007); $B_P = 5$ nT is the magnetic field at the edges of plasmoid. The configuration of the plasmoid can be seen in Figure 8.

We do not consider constant and uniform electric field in the system because we want to study acceleration effects produced by electromagnetic fluctuations. Our model is similar to the plasmoid configuration discussed by e.g. Tur et al. (2001), but its description is adapted to the observations in Jupiter's magnetotail. In the present paper, we do not consider self-consistent effects, that is, the influence of ion dynamics on the magnetic configuration of a plasmoid and its current sheet. The plasmoid is stationary.

In our model we consider the electromagnetic turbulence inside the plasmoid assuming that it is produced by an ensemble of electromagnetic fluctuations propagating in various directions with velocity $V_{PH} = \omega/\mathbf{k} \sim$ 650 km/s, which is close to local magnetosonic and Alfvén speeds (Kronberg, Woch, et al., 2008; Tao et al., 2015) and $\mathbf{k} = [k_X, k_Y, k_Z]$. The magnetic field fluctuations $\delta\mathbf{B} = (\delta B_X, \delta B_Y, \delta B_Z)$ have been taken as the sum of *N* harmonics

$$\delta\mathbf{B} = \sum_n^N B_n \cos(\mathbf{k}_n\mathbf{r} - \omega_n t + \phi_n).$$

Each harmonic has its own amplitude (B_n), wave number (k_n), frequency (w_n), and initial phase (ϕ_n). Frequencies and amplitudes of fluctuations were taken from the wavelet spectrum observed in the Jupiter's plasma sheet (Tao et al., 2015). The frequencies are taken in the range from 0.001 to 1 Hz. The power law slopes −1.36 and −2.52 below and above 0.01 Hz, respectively. ϕ_n is chosen randomly. Using the conditions of absence of free charge, the inductive electric field can be found from Maxwell equations

$$-\nabla \times \delta E = \frac{1}{c}\frac{\delta B}{\partial t}, \quad (2)$$

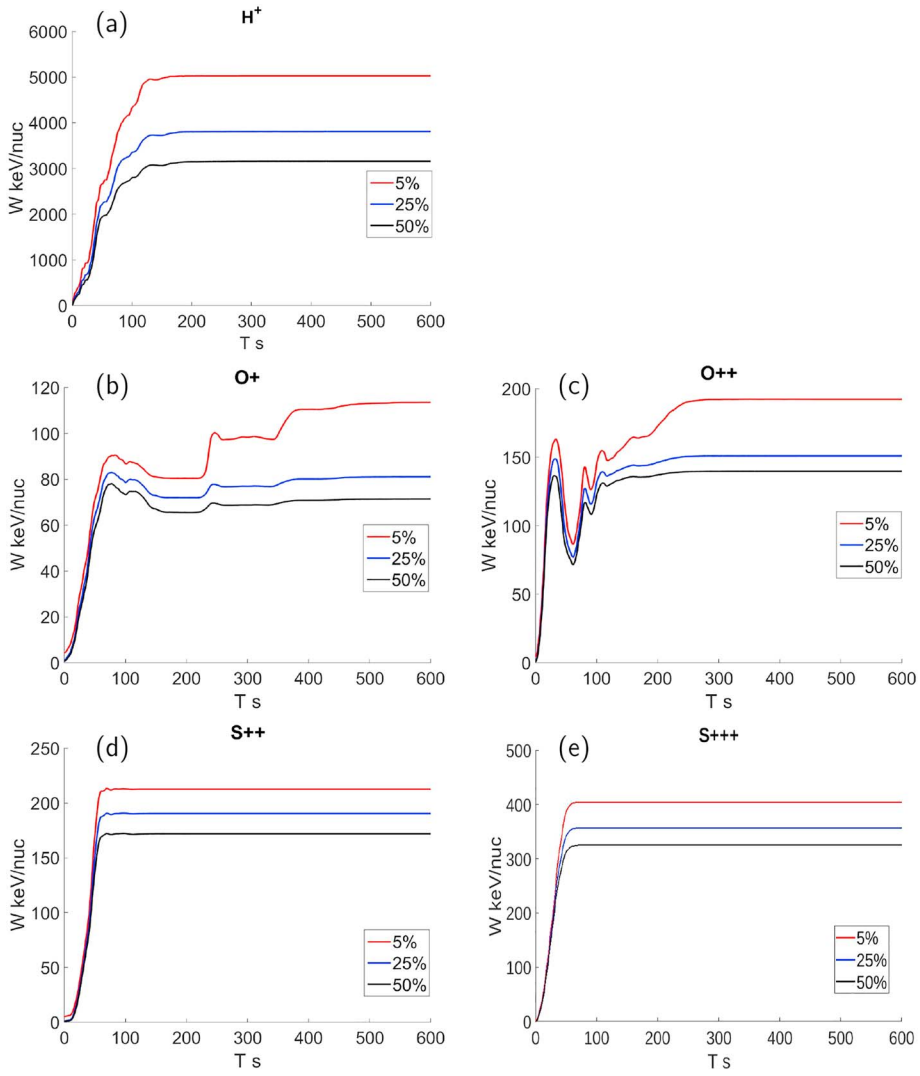

Figure 9. Energy gain versus time for ion populations representing the top 5% (red), 25% (blue), and 50% (black) of the particle energy and different species such as (a) H^+, (b) O^+, (c) O^{++}, (d) S^{++}, and (e) S^{+++}.

$$\nabla \delta E = 0. \tag{3}$$

We launched to the plasmoid 10^4 particles of H^+, O^+, O^{++}, S^{++}, and S^{+++} ions with Maxwell distributions and initial energies ~5 keV (Frank et al., 2002). We assume isotropic pitch angle distribution. The initial location of the particles in plasmoids and their trajectories are shown by circles in Figure 8.

We calculated the trajectories of particles in phase space of position and velocity and derived the evolution of the average energy of the top 5%, 25%, and 50% with respect to the particle energy. In addition, we calculated the energy distributions of particles in the time moments 0, 5, 50, 200, and 400 s from the launch.

Figure 9a shows that protons accelerate multiple times due to electromagnetic fluctuations during the first ~150 s. They leave the acceleration sites because of the increased velocity (the energy of the particles becomes constant when particles exit the zone of acceleration). The velocities of H^+ and $O^{+/++}$ are significantly different. Heavier ions are slower. Therefore, they resonantly interact with electromagnetic fluctuations during a longer time period, ~400 and ~200 s, for O^+ and O^{++}, respectively; see Figures 9b and 9c. The acceleration rate of O^+ ions is lower than of O^{++}. However, they spend a longer time in the acceleration site than O^{++}. Nevertheless, the maximum of the energy distribution at 400 s is higher for O^{++} ions; see Figure 10. The S^{++} and S^{+++} ions are resonantly accelerated during the first ~50 s and then leave the plasmoid; see Figures 9d and 9e. Sulfur ions, because of large gyroradii, leave the system relatively quickly.

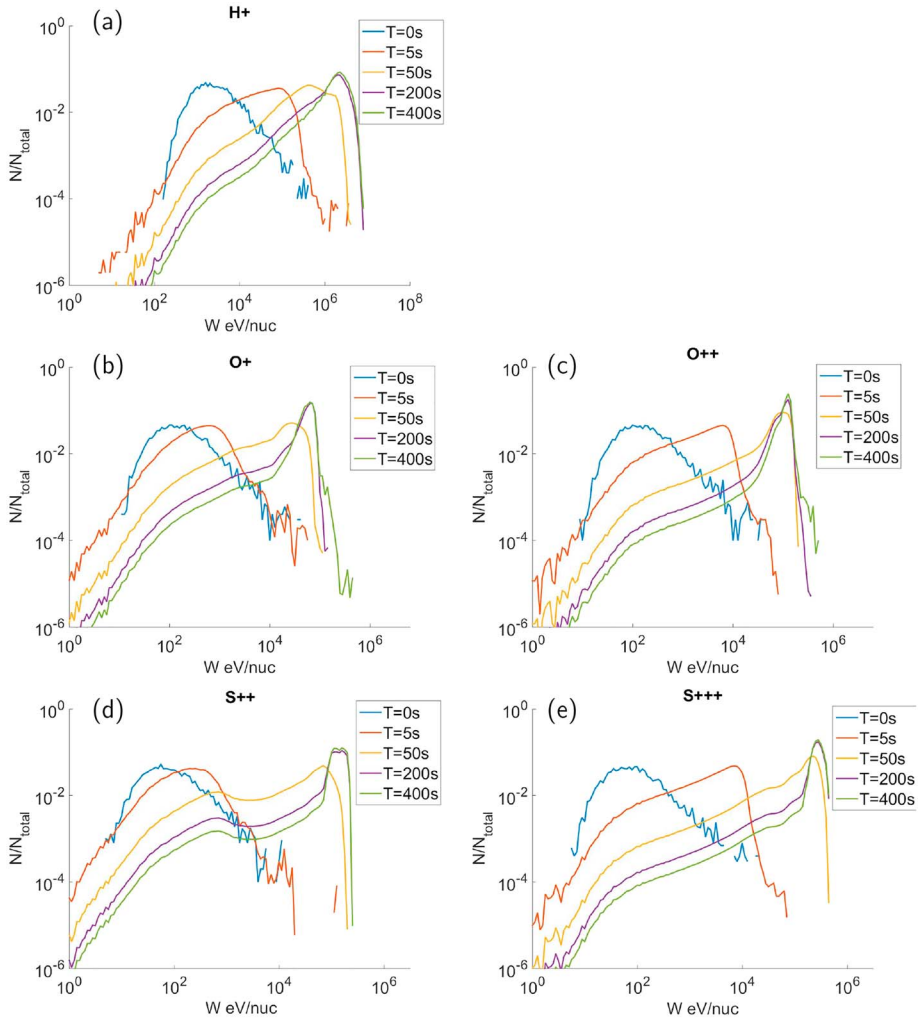

Figure 10. Energy distributions of the number of particles normalized to the total number of those at different time moments such as 0 s (blue), 5 s (red), 50 s (yellow), 200 s (violet), 400 s (green), and different species such as (a) H^+, (b) O^+, (c) O^{++}, (d) S^{++}, and (e) S^{+++}.

The acceleration of S^{++} ions is more efficient than that of O^{++} during a time interval of 400 s. It takes a less time and leads to higher energies. The most efficient acceleration is seen in S^{+++} ions. They get almost twice as much energy as S^{++} ions.

The evolution of energy distributions is shown in Figure 10 for H^+, O^+, O^{++}, S^{++}, and S^{+++} ions. Particles can be scattered by electromagnetic fluctuations; they can be accelerated and decelerated. In the figures one can see that the initial Maxwellian distributions at $t = 0$ s shift to higher energies with time. The process of acceleration is most significant after the first 5 s for S^{+++} and then for O^{++}. After ~50 s, the maximum of the ion energy distributions shifts to higher energies. This causes steeply falling tails in the energetic part of the spectra. In the Figure 10 one can see that ions with high charges are accelerated more.

The presence of powerful low-frequency turbulence can lead to the acceleration of heavy ions up to significantly high energies, E ~100–400 keV/nuc. The shape and the plasma properties of the Jovian magnetosphere allow us to extend our knowledge about the dynamics of charged particles and their interaction with electromagnetic turbulence.

5. Discussion

The results show that the oxygen and sulfur ion energization is correlated with the power of the magnetic field fluctuations at the frequency corresponding to f_{gi} of the O^+ and S^{++} ions. This result agrees with find-

ings by Radioti et al. (2007). They modeled the acceleration by time-varying electric field on the scales of the oxygen and sulfur gyrofrequency. Acceleration of oxygen and sulfur ions was significant and agreed with the observations. Hydrogen ions were not effectively accelerated by such electric field variations also in agreement with the observations. Generally, the wave power at H^+ on average is significantly lower (0.5 nT^2/Hz) than those at O^+ and S^{++} gyrofrequencies, 102 and 37 nT^2/Hz, respectively. Therefore, the resonant energy transfer from the electromagnetic fluctuations to hydrogen ions will lead to less effective acceleration.

In this study hydrogen ions at relatively high energies were investigated. Energy spectral index γ was calculated for energy channels 220–540 keV/nuc and 540 keV/nuc to 1,250 keV/nuc. The hydrogen intensity in both channels does not show any correlation with the wave power. The modeling in section 4 shows that the fast accelerated protons quickly leave the plasmoid. Therefore, it is possible that we do not observe the correlation of hydrogen ions at these energies with the wave power simply due to the time and energy resolution of our data. The most probable energy to be observed during 400 s is higher than our energy range (>2 MeV/nuc). S^{++} and S^{+++} also stop energy gain at comparable times; however, their most probable energy to be observed is about hundreds kiloelectron volts per nucleon. This is exactly the energy which we observe. Energy spectral index γ for oxygen calculated for energies at 76 and 251 keV/nuc (geometric means of the energy channels) does not show any correlation with the wave power at O^+ gyrofrequency (not shown). This implies that at higher energies ions do not interact effectively with waves presumably because of large ion gyroradius, and an upper limit should exist for an effective interaction. The upper limit approximately agrees with the upper limit predicted by the model for O^+ ions.

Comparison between the results of the present study and for the terrestrial plasmoids studied by Grigorenko et al. (2015) shows an agreement for oxygen ions. At both Earth and Jupiter the O^+ ions are effectively accelerated in plasmoids associated with strong turbulence. Even the level of turbulence required for effective acceleration is similar: wave power of the order of 10 nT^2Hz^{-1}. However, for hydrogen ions the results are different at Earth and Jupiter. In the similar range for the wave power at Jupiter no effective acceleration associated with turbulence is observed while at Earth it is seen. The model predicts their strong and fast acceleration. Therefore, the hydrogen ions may not be seen in the measured energy range and with given time resolution.

6. Conclusions

To investigate the transfer of the electromagnetic energy to the particle energy in this work, we used the multispecies ion observations from the EPD detector (H^+, oxygen and sulfur) in the energy range from 22 keV/nuc to 1,250 keV/nuc and magnetic field observations from the flux gate magnetometer onboard the Galileo spacecraft. We study 14 plasmoids observed in the Jovian magnetotail because in these structures especially strong ion acceleration is observed. We compare the results of observations with the test particle simulations. The simulations yield the kinetic features of ion trajectories in the prescribed plasmoid. Our results are the following: (1) The modeling predicts that electromagnetic turbulence in plasmoids plays an essential role in the acceleration of protons, oxygen, and sulfur ions. (2) Oxygen and sulfur intensities grow nonlinearly with the wave power at corresponding ion gyrofrequencies. The oxygen and sulfur energy spectral index γ at tens to hundreds kiloelectron volts per nucleon decreases with the wave power. These dependencies indicate an energy transfer from the electromagnetic waves to particles in agreement with the simulation results. The wave power threshold for acceleration is of the order of nT^2Hz^{-1}, as in terrestrial plasmoids. (3) In contrast, hydrogen intensity and energy spectral index γ at ~220 to ~1,250 keV/nuc do not show such correlations with the wave power as in (2) and as predicted by the model. This indicates that processes other than wave-particle interactions are responsible for the acceleration or that the time and energy resolution of the observations is too coarse. (4) The interaction of the waves and particles is nonlinear and requires further investigations, for example, of observations by the mission Juno.

Acknowledgments
This work was initiated at the ISSI team meeting on the "How does the Solar Wind Influence the Giant Planet Magnetospheres?" led M. Vogt and A. Masters. E. G., L. K., E. K., A. M., B. P., and H. M. are supported by the Volkswagen foundation under Grant 90 312. M. F. V. was supported by the National Science Foundation under award 1524651 and by the National Aeronautics and Space Administration under Grant 80NSSC17K0733. We thank N. Krupp for useful discussions. The Galileo data can be found at the Planetary Data System (https://pds.nasa.gov/). The data analysis was done with Python and SciPy.

References

Bagenal, F., & Delamere, P. A. (2011). Flow of mass and energy in the magnetospheres of Jupiter and Saturn. *Journal of Geophysical Research*, *116*, A05209. https://doi.org/10.1029/2010JA016294

Catapano, F., Zimbardo, G., Perri, S., Greco, A., & Artemyev, A. V. (2016). Proton and heavy ion acceleration by stochastic fluctuations in the Earth's magnetotail. *Annales Geophysicae*, *34*, 917–926. https://doi.org/10.5194/angeo-34-917-2016

Clark, G., Mauk, B. H., Paranicas, C., Kollmann, P., & Smith, H. T. (2016). Charge states of energetic oxygen and sulfur ions in Jupiter's magnetosphere. *Journal of Geophysical Research: Space Physics*, *121*, 2264–2273. https://doi.org/10.1002/2015JA022257

Delcourt, D. C., & Sauvaud, J. A. (1994). Plasma sheet ion energization during dipolarization events. *Journal of Geophysical Research*, *99*, 97–108. https://doi.org/10.1029/93JA01895

Frank, L. A., Paterson, W. R., & Khurana, K. K. (2002). Observations Of thermal plasmas in Jupiter's magnetotail. *Journal of Geophysical Research*, *107*(A1), 1003. https://doi.org/10.1029/2001JA000077

Geiss, J., Gloeckler, G., Balsiger, H., Fisk, L. A., Galvin, A. B., Gliem, F., et al. (1992). Plasma composition in Jupiter's magnetosphere—Initial results from the solar wind ion composition spectrometer. *Science*, *257*, 1535–1539.

Goedbloed, H., & Poedts, S. (2004). *Principles of magnetohydrodynamics* (pp. 587). Cambridge: Cambridge University.

Greco, A., Artemyev, A., & Zimbardo, G. (2015). Heavy ion acceleration at dipolarization fronts in planetary magnetotails. *Geophysical Research Letters*, *42*, 8280–8287. https://doi.org/10.1002/2015GL066167

Grigorenko, E. E., Kronberg, E. A., & Daly, P. W. (2017). Heating and acceleration of charged particles during magnetic dipolarizations. *Cosmic Research*, *55*, 57–66. https://doi.org/10.1134/S0010952517010063

Grigorenko, E. E., Malykhin, A. Y., Kronberg, E. A., Malova, K. V., & Daly, P. W. (2015). Acceleration of ions to suprathermal energies by turbulence in the plasmoid-like magnetic structures. *Journal of Geophysical Research: Space Physics*, *120*, 6541–6558. https://doi.org/10.1002/2015JA021314

Gurnett, D. A., Kurth, W. S., Shaw, R. R., Roux, A., Gendrin, R., Kennel, C. F., et al. (1992). The galileo plasma wave investigation. *Space Science Reviews*, *60*, 341–355. https://doi.org/10.1007/BF00216861

Haggerty, D. K., Hill, M. E., McNutt, R. L., & Paranicas, C. (2009). Composition of energetic particles in the Jovian magnetotail. *Journal of Geophysical Research*, *114*, A02208. https://doi.org/10.1029/2008JA013659

Kasahara, S., Kronberg, E. A., Krupp, N., Kimura, T., Tao, C., Badman, S. V., et al. (2011). Magnetic reconnection in the Jovian tail: X-line evolution and consequent plasma sheet structures. *Journal of Geophysical Research*, *116*, A11219. https://doi.org/10.1029/2011JA016892

Khurana, K. K., & Kivelson, M. G. (1989). On Jovian plasma sheet structure. *Journal of Geophysical Research*, *94*(13), 11,791–11,803.

Kivelson, M. G., Khurana, K. K., Means, J. D., Russell, C. T., & Snare, R. C. (1992). The Galileo magnetic field investigation. *Space Science Reviews*, *60*, 357–383.

Kronberg, E. A., Glassmeier, K.-H., Woch, J., Krupp, N., Lagg, A., & Dougherty, M. K. (2007). A possible intrinsic mechanism for the quasi-periodic dynamics of the Jovian magnetosphere. *Journal of Geophysical Research*, *112*, A05203. https://doi.org/10.1029/2006JA011994

Kronberg, E. A., Glassmeier, K.-H., Woch, J., Krupp, N., Lagg, A., & Dougherty, M. K. (2008). Comparison of periodic substorms at Jupiter and Earth. *Journal of Geophysical Research*, *113*, A04212. https://doi.org/10.1029/2007JA012880

Kronberg, E. A., Kasahara, S., Krupp, N., & Woch, J. (2012). Field-aligned beams and reconnection in the Jovian magnetotail. *Icarus*, *217*, 55–65. https://doi.org/10.1016/j.icarus.2011.10.011

Kronberg, E. A., Welling, D., Kistler, L. M., Mouikis, C., Daly, P. W., Grigorenko, E. E., et al. (2017). Contribution of energetic and heavy ions to the plasma pressure: The 27 September to 3 October 2002 storm. *Journal of Geophysical Research: Space Physics*, *122*, 9427–9439. https://doi.org/10.1002/2017JA024215

Kronberg, E. A., Woch, J., Krupp, N., & Lagg, A. (2008). Mass release process in the Jovian magnetosphere: Statistics on particle burst parameters. *Journal of Geophysical Research*, *113*, A10202. https://doi.org/10.1029/2008JA013332

Kronberg, E. A., Woch, J., Krupp, N., & Lagg, A. (2009). A summary of observational records on periodicities above the rotational period in the Jovian magnetosphere. *Annales Geophysicae*, *27*, 2565–2573. https://doi.org/10.5194/angeo-27-2565-2009

Kronberg, E. A., Woch, J., Krupp, N., Lagg, A., Khurana, K. K., & Glassmeier, K.-H. (2005). Mass release at Jupiter: Substorm-like processes in the Jovian magnetotail. *Journal of Geophysical Research*, *110*, A03211. https://doi.org/10.1029/2004JA010777

Krupp, N., Lagg, A., Livi, S., Wilken, B., Woch, J., Roelof, E. C., & Williams, D. J. (2001). Global flows of energetic ions in Jupiter's equatorial plane: First-order approximation. *Journal of Geophysical Research*, *106*(15), 26,017–26,032.

Luo, H., Kronberg, E. A., Grigorenko, E. E., Fränz, M., Daly, P. W., Chen, G. X., et al. (2014). Evidence of strong energetic ion acceleration in the near-Earth magnetotail. *Geophysical Research Letters*, *41*, 3724–3730. https://doi.org/10.1002/2014GL060252

Lyons, L. R., & Speiser, T. W. (1982). Evidence for current sheet acceleration in the geomagnetic tail. *Journal of Geophysical Research*, *87*, 2276–2286. https://doi.org/10.1029/JA087iA04p02276

Malykhin, A. Y., Grigorenko, E. E., Kronberg, E. A., Koleva, R., Ganushkina, N. Y., Kozak, L., & Daly, P. W. (2018). Contrasting dynamics of electrons and protons in the near-Earth plasma sheet during dipolarization. *Annales Geophysicae*, *36*, 741–760. https://doi.org/10.5194/angeo-36-741-2018

Nakamura, R., Baumjohann, W., Mouikis, C., Kistler, L. M., Runov, A., Volwerk, M., et al. (2004). Spatial scale of high-speed flows in the plasma sheet observed by cluster. *Geophysical Research Letters*, *31*, L09804. https://doi.org/10.1029/2004GL019558

Ono, Y., Nosé, M., Christon, S. P., & Lui, A. T. Y. (2009). The role of magnetic field fluctuations in nonadiabatic acceleration of ions during dipolarization. *Journal of Geophysical Research*, *114*, A05209. https://doi.org/10.1029/2008JA013918

Parkhomenko, E. I., Malova, H. V., Grigorenko, E. E., Popov, V. Y., Petrukovich, A. A., Delcourt, D. C., et al. (2018). Plasma acceleration on multiscale temporal variations of electric and magnetic fields during substorm dipolarization in the Earth's magnetotail. *Annals of Geophysics*, *61*, GM334. https://doi.org/10.4401/ag-7582

Radioti, A., Woch, J., Kronberg, E. A., Krupp, N., Lagg, A., Glassmeier, K.-H., & Dougherty, M. K. (2007). Energetic ion composition during reconfiguration events in the Jovian magnetotail. *Journal of Geophysical Research*, *112*, A06221. https://doi.org/10.1029/2006JA012047

Richardson, I. G., Cowley, S. W. H., Hones, E. W. Jr, & Bame, S. J. (1987). Plasmoid-associated energetic ion bursts in the deep geomagnetic tail - properties of plasmoids and the postplasmoid plasma sheet. *Journal of Geophysical Research*, *92*, 9997–10,013. https://doi.org/10.1029/JA092iA09p09997

Tao, C., Sahraoui, F., Fontaine, D., Patoul, J., Chust, T., Kasahara, S., & Retinò, A. (2015). Properties of Jupiter's magnetospheric turbulence observed by the galileo spacecraft. *Journal of Geophysical Research: Space Physics*, *120*, 2477–2493. https://doi.org/10.1002/2014JA020749

Torrence, C., & Compo, G. P. (1998). A practical guide to wavelet analysis. *Bulletin of the American Meteorological Society*, *79*, 61–78. https://doi.org/10.1175/1520-0477(1998)079<0061:APGTWA>2.0.CO;2

Tur, A., Louarn, P., Yanovsky, V., Le Queau, D., & Genot, V. (2001). On the asymptotic theory of localized structures in a thin two-dimensional Harris current sheet: Plasmoids, multiplasmoids and x points. *Journal of Plasma Physics*, *66*, 97–117. https://doi.org/10.1017/S002237780100112X

Vasyliūnas, V. M. (1983). Plasma distribution and flow, *Physics of the Jovian magnetosphere* (pp. 395–453). Cambridge: Cambridge University Press.

Vogt, M. F., Jackman, C. M., Slavin, J. A., Bunce, E. J., Cowley, S. W. H., Kivelson, M. G., & Khurana, K. K. (2014). Structure and statistical properties of plasmoids in Jupiter's magnetotail. *Journal of Geophysical Research: Space Physics*, *119*, 821–843. https://doi.org/10.1002/2013JA019393

Williams, D. J., McEntire, R. W., Jaskulek, S., & Wilken, B. (1992). The Galileo energetic particles detector. *Space Science Reviews*, *60*, 385–412.

Woch, J., Krupp, N., Khurana, K. K., Kivelson, M. G., Roux, A., Perraut, S., et al. (1999). Plasma sheet dynamics in the Jovian magnetotail: Signatures for substorm-like processes? *Geophysical Research Letters*, *26*, 2137–2140.

Woch, J., Krupp, N., Lagg, A., Wilken, B., Livi, S., & Williams, D. J. (1998). Quasi-periodic modulations of the Jovian magnetotail. *Geophysical Research Letters*, *25*, 1253–1256.

Wygant, J. R., Cattell, C. A., Lysak, R., Song, Y., Dombeck, J., McFadden, J., et al. (2005). Cluster observations of an intense normal component of the electric field at a thin reconnecting current sheet in the tail and its role in the shock-like acceleration of the ion fluid into the separatrix region. *Journal of Geophysical Research*, *110*, A09206. https://doi.org/10.1029/2004JA010708

Zong, Q.-G., Wilken, B., Reeves, G. D., Daglis, I. A., Doke, T., Iyemori, T., et al. (1997). Geotail observations of energetic ion species and magnetic field in plasmoid-like structures in the course of an isolated substorm event. *Journal of Geophysical Research*, *102*, 11,409–11,428. https://doi.org/10.1029/97JA00076